Measurement of the silver freezing point with an optical fiber thermometer: Proof of concept

R. R. Dils,[a] J. Geist, and M. L. Reilly
National Bureau of Standards, Gaithersburg, Maryland 20899

(Received 23 July 1985; accepted for publication 6 November 1985)

Measurements were made at the gold and silver freezing points to demonstrate the accuracy of the new optical fiber thermometer (OFT). It is shown that the output signal from the OFT is related to the radiance from a blackbody source in a simple manner and that the temperature interval between the gold and silver freezing points, as determined with the OFT, is close to other recent results.

I. INTRODUCTION

An optical fiber thermometer (OFT) suitable for temperature measurements in the range 600–2000 °C has been described recently[1]; its concept and design are straightforward. A metallic blackbody cavity is sputtered on the tip of a single-crystal fiber of sapphire. When the cavity is heated, its radiance in a narrow wavelength band is used to determine its temperature. The high-temperature sapphire fiber and a low-temperature silica glass fiber transmit the signal to an interference filter and optical detector. The performance analyses predict the potential temperature sensitivity and accuracy of the OFT to be extraordinary.

The experiments reported in the original paper[1] demonstrated that temperatures in the range 700–1000 °C could be measured with an uncertainty on the order of $\pm 0.05\%$. Although the accuracy was limited in part by the OFT design, a major source of error appeared to be the uncertainty of the temperatures derived from thermocouple measurements. It has been estimated[2] that the minimum uncertainty in a single determination of an unknown temperature measured with a platinum-10% rhodium versus platinum thermocouple, which has just been calibrated on the International Practical Temperature Scale of 1968 (IPTS-68),[3] is ± 0.2 °C near 1000 °C. Furthermore, it is well known that the thermal history of a thermocouple affects its performance in a complicated way that can increase the uncertainty many tenths of a kelvin above this minimum level.[4]

This paper describes measurements made at the freezing point of silver and the freezing point of gold to test further the accuracy of the OFT. The temperature at each freezing point is known to be highly reproducible and the temperature interval between the two freezing points has been determined by a number of investigators.[5–12] It is shown that the output signal from the OFT is related to the radiance from a blackbody source in a simple manner and that the temperature interval between the gold and silver freezing points, as determined with the OFT, is close to other recent results. These measurements were completed in February 1983.

II. EXPERIMENTAL APPARATUS

The general experimental arrangement of the freezing-point cell and the OFT is shown in Fig. 1. The freezing-point cell, the lower portion of the probe, and Al_2O_3 fiber of the OFT are drawn to the same scale. The components of the radiometer portion of the OFT are shown schematically.

A. Gold and silver freezing-point cells

The gold and silver freezing points were realized in sealed cells. The fused-quartz glass envelope of each cell en-

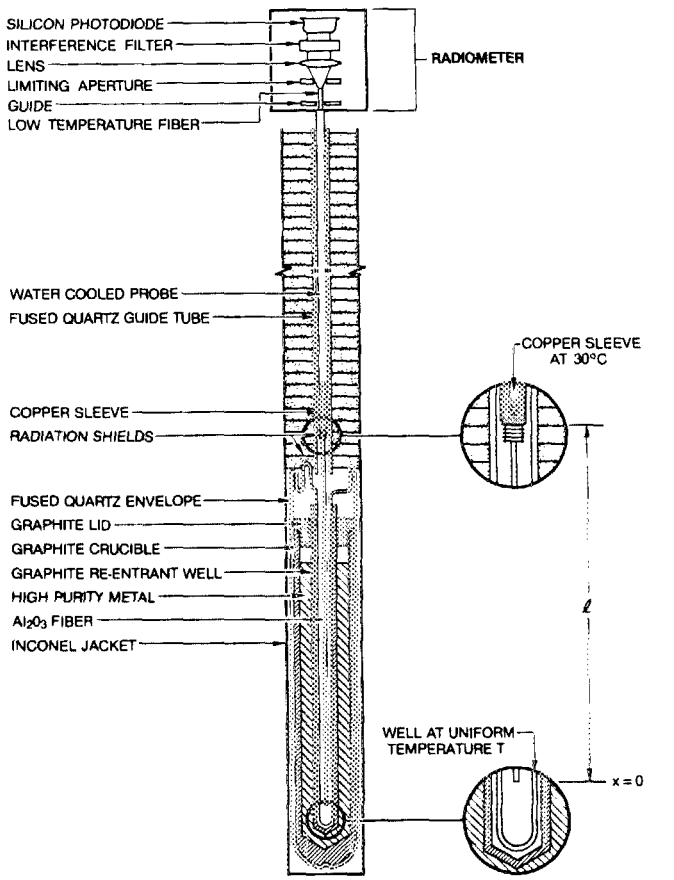

FIG. 1. Experimental arrangement showing details of the freezing-point cell and the optical fiber thermometer as used in this experiment. The inconel jacket is surrounded by an electrically heated furnace which is used to control the melting and freezing of the metal in the cell.

[a] Present address: Accufiber Corporation, 2000 E. Columbia Way, Bldg. 7, Vancouver, WA 98664.

 0021-8979/86/041005-08$02.40

closed the high-purity metal which was contained within a cylindrical graphite crucible closed by a lid having a graphite reentrant thermometer well. After a freeze was initiated, the temperature over the lower part of the well remained constant to within a few millikelvins. From freeze to freeze the temperature, as determined by platinum resistance thermometry, was reproducible to within approximately ± 0.002 °C.[13] For this experiment, the glass-lined thermometer well of the freezing-point cell was assumed to be a blackbody cavity. The inner diameter of the well was 6 mm. The distance from the top of the liquid metal to the inside bottom of the well was about 17 cm for the silver cell and about 15 cm for the gold cell. The freezing-point cells and their associated furnaces were designed for testing the performance of high-temperature long-stem platinum resistance thermometers. As a consequence, the bottom of the thermometer well was more than 50 cm below the top surface of the furnance.

B. Optical fiber thermometer

The optical fiber thermometer (OFT) used in these freezing-point experiments differed from that used in the previous experiments[1] in several significant features: (1) A silicon photodiode was used as the detector in place of a photomultiplier tube. (2) Only a single compound interference filter was used without any beamsplitter or neutral density filters. (3) The high-temperature fiber *did not* have a blackbody cavity coating on its tip.

The high-temperature fiber of the OFT was a 1.25-mm-diam, 23-cm-long single crystal of sapphire (α-Al_2O_3) with the cylindrical axis parallel to the c axis of the crystal. The crystal was commerically grown by the method of edge-defined film-fed growth.[14,15] Both end faces of the uncoated fiber were cut and polished at an angle of 90° to its axis.

Because the depth of immersion required by the freezing-point furnances exceeded the length of the sapphire fiber, it was necessary to build a probe which extended down into the guide tube above the cell in order to (a) place the sapphire fiber in an isothermal region and reproducibly position its tip approximately 2.5 cm above the bottom of the well of the freezing-point cell, and (b) provide a water-cooled mechanical coupling between the high- and low-temperature fibers as well as a cool environment for the low-temperature fiber which passed up through the center of the probe. The upper end of the probe was mechanically attached to the radiometer housing and support.

The low-temperature fiber was a 0.6-mm-diam silica-core, step-index, silicon-clad fiber covered with a protective plastic sheath.

The high-temperature sapphire fiber and the low-temperature transmitting fiber were butted together inside a short length (~ 1 cm) of close-fitting glass tubing and were fixed in place with epoxy cement. The glass tubing was held in the water-cooled copper sleeve, located at the lower end of the probe, by means of a set screw and Teflon pad which pressed the tube against the inner surface of the sleeve.

The probe was cooled with water from a temperature regulated recirculating supply. The water temperature was nominally set at 25 °C but varied in a regular manner between 23.6 and 26.4 °C during the 3.2-min regulation cycle. This temperature excursion caused an expansion and contraction of several micrometers in the 60-cm length of the probe. During initial testing, the upper end of the low-temperature fiber was also held in a fixed position at the radiometer. However, the attendant dimensional changes were sufficient to cause regular periodic variations in the output of the radiometer which were attributed to stress-induced variation in the optical transmission through the low-temperature fiber. To minimize this effect, the optic element formed by the sapphire plus low-temperature fiber was fixed only at the copper sleeve while its upper end was allowed to slide freely through a guide located in front of the limiting aperture of the radiometer.

The radiometer was of conventional design and was built with readily available optical and electronic components throughout. As shown in Fig. 1, the radiant flux exiting the low-temperature fiber was limited by an aperture, collected with a lens and focused through a compound, narrow-band interference filter (800-nm peak wavelength with a 100-nm bandpass) onto a silicon photodiode. The aperture was introduced to restrict the flux to near normal components (the numerical aperture was approximately 0.1) and thereby (1) reduce the effects due to the movement of the free end of the low-temperature fiber relative to the aperture, (2) limit the effects of the dependence of wide-angle rays upon induced stress in the low-temperature fiber, and (3) provide for optimum performance of the interference filter.

III. MEASUREMENTS AT THE GOLD AND SILVER FREEZING POINTS

Initially, each furnace was held about 10 °C above the freezing temperature to completely melt the metal in the freezing-point cell. With the OFT in place, the furnance was then set to control at a temperature just below the freezing point. The output of the OFT was recorded for 50 min beginning as the liquid metal approached its freezing point. Within about 30 min after recalescence occurred (with the corresponding sudden increase in temperature) the cell reached an isothermal state and the freezing point was realized.

The output signal from the OFT during such a measurement sequence is shown in Fig. 2 for measurements at the silver freezing point and in Fig. 3 for measurements at the gold freezing point. For convenience, the output signal is expressed as a temperature difference relative to an arbitrary reference temperature. A reproducible periodic variation in the signal is clearly evident in both figures. (The beginning of each period was directly correlated with the start of the refrigeration portion of the regulation cycle of the water supply.)

Figure 4 shows the output signal, obtained at the silver freezing point during an initial test, when the OFT was equipped with a fiber optic element constructed from three individual Al_2O_3 fibers joined end to end. An indication of the contribution of the low-temperature fiber can be seen by comparing the signal shown in Fig. 2, obtained when the OFT was equipped with the Al_2O_3 plus low-temperature fiber combination previously described, with that shown in Fig. 4. The periodic variation in Fig. 4 is also due to contraction and expansion of the water-cooled probe and the atten-

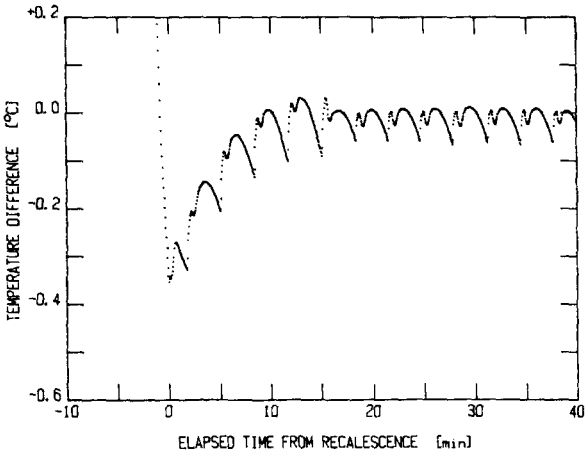

FIG. 2. Output signal from the optical fiber thermometer recorded during measurements in the silver freezing-point cell. For convenience, the output signal is expressed as a temperature difference relative to an arbitrary reference temperature. The periodic variation was caused by the temperature regulation cycle of the cooling water flowing through the probe (see discussion in text).

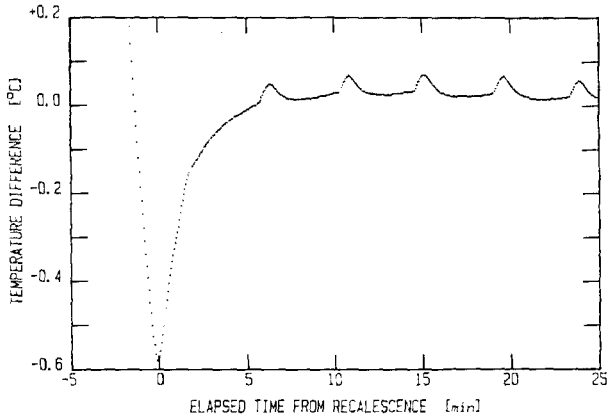

FIG. 4. Output signal from the optical fiber thermometer recorded during a test measurement in the silver freezing-point cell. For convenience, the output signal is expressed as a temperature difference relative to an arbitrary reference temperature. These data were obtained when the OFT was equipped with an optic element constructed from three individual Al_2O_3 fibers joined end to end. Note the difference between the shape of the periodic variation in this figure and that obtained when the OFT was equipped with the combination Al_2O_3 plus low-temperature fiber element (Figs. 2 and 3).

dant motion of the upper end of the low-temperature fiber relative to the limiting aperture of the radiometer. With both configurations, the variation in the output signal was correlated with the regulation cycle of the water supply.

The periodic variation of the output signal from the OFT did not preclude the use of the data. At the silver freezing point (Fig. 2), the peak-to-peak change was 8×10^{-4} of the total output signal; at the gold freezing point (Fig. 3), the corresponding peak-to-peak change was 18×10^{-4}. This variation was found to be quite reproducible. For the last four periods of data obtained at the silver freezing point, the magnitude of the OFT output at the same distinctive point within each period (e.g., at the broad maximum) was reproducible within $\pm 0.5\times10^{-4}$ of the signal. Equivalent reproducibility of corresponding points was also found for the last four periods of the data obtained at the gold freezing point. These results confirm that each cell had reached an isothermal state. The last four periods of the data obtained at the gold and silver freezing points were used to calculate an experimental value of 2.9995 for the ratio of the radiance at the gold point to that at the silver point. From the range of differences between the ratios at the corresponding points, the systematic error in the experimental ratio was estimated to be ± 0.0006 ($\pm 0.02\%$).

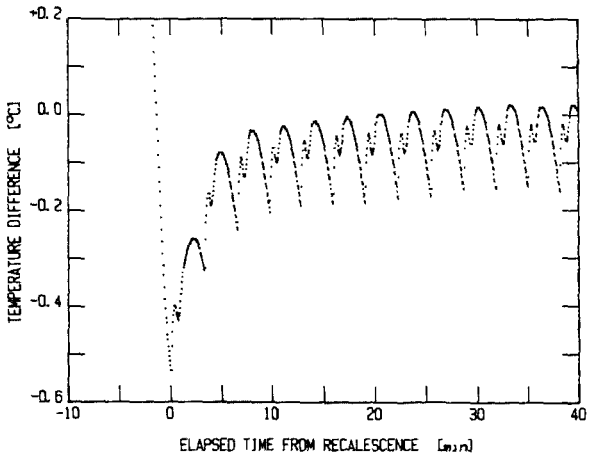

FIG. 3. Output signal from the optical fiber thermometer recorded during measurements in the gold freezing-point cell. For convenience, the output signal is expressed as a temperature difference relative to an arbitrary reference temperature. The periodic variation was caused by the temperature regulation cycle of the cooling water flowing through the probe (see discussion in text).

IV. AUXILIARY MEASUREMENTS

In addition to the unknown error in the value assigned to the temperature of the gold point, there are three major sources of error that limit the accuracy with which the OFT can be used to determine thermodynamic temperature. These are (1) uncertainties in the spectral response characteristics of the optical system (particularly the interference filter and the detector), (2) uncertainties in the linearity of the detector and its associated electronic circuitry, and (3) uncertainties in the optical properties of the high-temperature fiber. In this section independent measurements of the spectral response and linearity of the OFT radiometer plus measurements of the magnitude and temperature dependence of absorption and scattering in the sapphire fiber are briefly described.

A. Transmission of the narrow-band interference filter

The spectral transmittance $\tau(\lambda)$ of the narrow-band interference filter (800-nm peak wavelength with a 100-nm bandpass) was measured over its bandpass on the NBS high-accuracy spectrophotometer[16] with a wavelength accuracy of ± 0.04 nm; the out-of-band transmittance was measured with a CARY Model 14 spectrophotometer. The results are shown in Fig. 5. The nominal spectral response $r(\lambda)$ of the silicon photodiode is also presented in Fig. 5.

The dashed lines on the $\tau(\lambda)$ curve are estimated upper bounds in the spectral regions where the CARY spectropho-

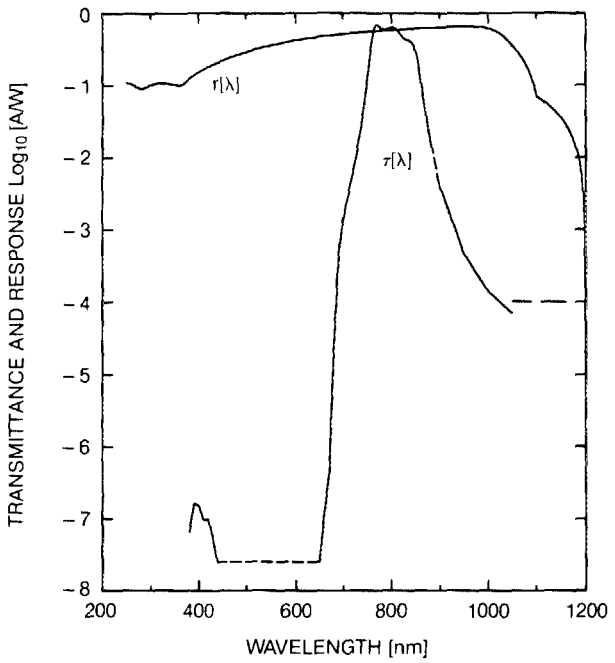

FIG. 5. Spectral transmittance $\tau(\lambda)$ of the narrow-band interference filter (800-nm peak wavelength with 100-nm bandpass) used in this experiment. Also shown is the nominal spectral response $r(\lambda)$ of the silicon photodiode.

tometer was not sensitive enough to detect the radiation transmitted through the filter. The shoulder on the $r(\lambda)$ curve beyond 1100 nm is an estimate of an upper bound to the response associated with the absorption of sub-band-gap photons by transitions from the top of the valence band to donor ions in the n-type region of the p^+nn^+ photodiode. This extrapolation passes through the measured response at the 1150-nm HeNe laser line.

From these measurements it was possible to define $\tau(\lambda)$ with an uncertainty of $\pm 0.0041\%$ due to wavelength accuracy and $\pm 0.0032\%$ due to out-of-bound transmissions; these lead to corrections of $0 \pm 0.005\,^{\circ}\mathrm{C}$ and $-0.004 \pm 0.004\,^{\circ}\mathrm{C}$ in the silver freezing-point temperature, respectively. Note that it is only the shape of the pass band, not the absolute transmittance, that enters into these calculations.

B. Electronic circuitry

The silicon photodiode was operated in the photoamperic mode and the induced photocurrent was measured with a high-input-impedance, high-gain amplifier, and bandpass circuit. The electronic circuit was found to be linear within 1.88×10^{-5} from 10^{-8} to 10^{-6} A, which included the photocurrent range of the measurements at the gold and silver freezing points. The electronic noise was $3.87\times10^{-14}\sqrt{f}$ A, which is a factor of 4 smaller than the shot noise associated with a photon flux causing a 10^{-7} A photocurrent. The electronic drift was 3.85×10^{-14} A h^{-1}. These values correspond to uncertainties of $\pm 0.0017\,^{\circ}\mathrm{C}$, $\pm 0.00003\sqrt{f}\,^{\circ}\mathrm{C}$, and $\pm 0.00003\,^{\circ}\mathrm{C\,h^{-1}}$, respectively, in the silver freezing-point temperature. When compared with the other sources of error described below, negligible error was introduced by the electronic circuit.

C. Radiometric nonlinearity

The linearity of the radiometer response was measured using a common technique[17] with the apparatus that is sketched in Fig. 6. The radiation from a Quinn–Lee[18] tungsten strip lamp passed through two apertures, A and B, in an opaque screen onto a lens which imaged the filament of the strip lamp onto one end of the low-temperature optical fiber. The other end of the fiber was mounted in the radiometer. A shutter was positioned near each aperture in such a way that the apertures could be opened or closed independently.

The apparatus shown in Fig. 6 has four states. The radiometer output voltages corresponding to these four states are $V(\phi_0)$, $V(\phi_A)$, $V(\phi_B)$, and $V(\phi_{A+B})$. Here $V(\phi_i)$ represents the radiometer output voltage when radiation flux ϕ_i is incident on the end of the optical fiber. The subscripts 0, A, B, and $A+B$ correspond to the states (1) both shutters closed, (2) only shutter A open, (3) only shutter B open, and (4) both shutters open, respectively. Thus if the ratio

$$R_L = \frac{V(\phi_A) - V(\phi_0) + V(\phi_B) - V(\phi_0)}{V(\phi_{A+B}) - V(\phi_0)} \tag{1}$$

is unity, the radiometer output voltage is linearly related to the flux incident on the fiber tip. Of course, if R_L is not unity, it can be used to derive a correction for the nonlinear response of the radiometer.

R_L was determined as a function of output voltage for photocurrents ranging from 3×10^{-8} to 8×10^{-7} A. Although the lamp current was feedback stabilized using an air cooled shunt resistor, the flux from the tungsten strip lamp drifted on the order of a few parts in 10^4 during the measurement interval. To compensate for this, $V(\phi_{A+B})$ was measured at the beginning and end of each interval.

The total error due to nonlinearity is estimated to be approximately 1×10^{-4}. Figure 7 shows the nonlinearity data over the output voltage range that applied to the measurements at the silver and gold freezing points. Note that the sum of the individual readings was always larger than $V(\phi_{A+B})$.

The measured nonlinearity may be an artifact of the linearity measurement technique rather than a defect in the photodiode or in the electronic circuit. This possibility must be taken into account when estimating the uncertainty of correction factors based on the data shown in Fig. 7.

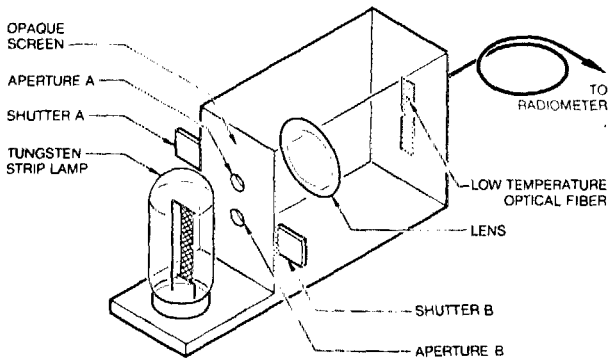

FIG. 6. A sketch of the apparatus used for the determination of the radiometer linearity.

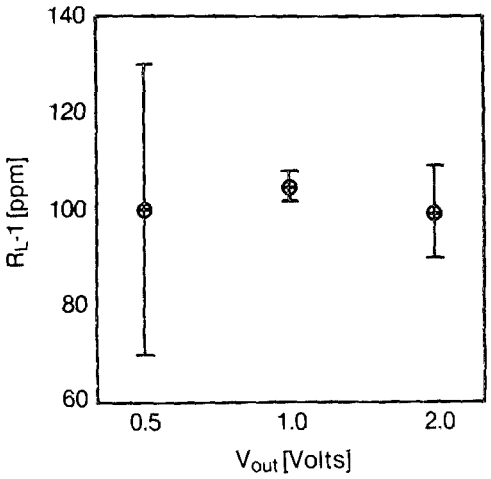

FIG. 7. Observed linearity data for the radiometer when equipped with the 800-nm narrow-band interference filter used in this experiment.

To derive $V(\phi)$ from these results, we assume that the radiometer response can be represented by the following relationship which distributes the nonlinearity uniformly over the measurement range

$$V(\phi) = V(\phi_0) + K\,(\phi/\phi_1)^N, \tag{2}$$

where $V(\phi_1) = V(\phi_0) + K$ and N is an exponent to be determined from the data. Then by substituting Eq. (2) into Eq. (1), we obtain

$$R_L = \frac{(\phi_A)^N + (\phi_B)^N}{(\phi_A + \phi_B)^N} = (2.05)^{1-N}, \tag{3}$$

because $V(\phi_B) = 1.05 \times V(\phi_A)$ for the linearity apparatus.

To allow both for the imprecision in the data of Fig. 7 and for the possibility that the systematic difference between R_L and unity was an artifact of the linearity apparatus, we assumed that $1.000\,00 < R_L < 1.000\,13$, from which we obtained $0.999\,82 < N < 1.000\,00$. Thus we adopted Eq. (2) with $N = 0.999\,91 \pm 0.000\,09$ as our model of the radiometer input-output relation. For the ratio of the radiance measured at the gold point to that measured at the silver point, the correction for the nonlinearity of the radiometer response corresponds to 0.009 ± 0.009 °C in the silver freezing-point temperature.

D. Absorption and scattering in the high-temperature sapphire fiber

In order to know the relation between the radiation leaving the high-temperature fiber and the temperature of the fiber tip blackbody environment which is provided by the freezing-point cell, it is necessary to solve the equations of radiative transfer for the geometry detailed in Fig. 1. Because the index of refraction of Al_2O_3 is high and the solid angle collected by the radiometer optics is small, the problem reduces to a one dimensional transfer along the axis of the fiber. Negligible flux is lost through scattering due to the uniform temperature (blackbody) radiation environment in which the fiber is immersed. As a result, the spectral distribution of the flux in the direction of the radiometer at a distance l from the tip of the Al_2O_3 fiber is given by

$$\phi(l) = \phi_{BB}(T)\,\{1-\rho[T(0)]\}\exp\left(-\int_0^l \alpha[T(s)]ds\right) + \int_0^l dx\,\alpha[T(x)]\,\phi_{BB}[T(x)] \times \exp\left(-\int_x^l \alpha[T(s)]ds\right) + \cdots, \tag{4}$$

where $\phi_{BB}(T)$ is the Planck function evaluated at the temperature T of the well of the freezing-point cell, $\rho[T(0)]$ is the reflectance of the fiber tip as a function of the temperature $T(0)$ of the fiber tip, and $\alpha[T(x)]$ is the absorption coefficient of the fiber at the point x at the temperature $T(x)$.

Several experiments were conducted to characterize the absorption and scattering in a number of sapphire fibers. These measurements were conducted in a free stream of hot exhaust gas which was generated in a laboratory combustor. The combustor has been described previously.[19–21] The mass rate of flow of the exhaust gas was maintained at 8.4 kg min^{-1} in a 7.6-cm cylindrical exhaust nozzle; the fuel flow was adjusted to vary the gas temperature from 850 to 1060 °C. The velocity of the gas stream varied from 210 m s^{-1} at 850 °C to 250 m s^{-1} at 1060 °C. At an average gas temperature of 1093 °C and velocity of 304 m s^{-1}, the temperature distribution across a typical radial traverse of the gas stream at the exhaust nozzle had been found to be uniform to within $\pm 1\%$.[20] This unusual source of heat was used in order to heat the fiber without exposing it to a significant source of radiant flux, thus enabling the weak self-emission from the fiber to be measured.

The sapphire fiber of the OFT was placed across the exhaust stream 3.2 cm downstream from the nozzle and perpendicular to the axis of flow. The tip of the fiber extended beyond the boundary of the flow so that the acceptance angle of the fiber included only room-temperature radiation sources. The central 7.6-cm section of the fiber was heated to the temperature of the exhaust stream while the output of the OFT was recorded.

The light originating in the forward sections of the combustor was blocked with a 4.8-mm-diam ceramic rod which was placed 6.4 mm upstream from and parallel to the fiber. The temperature of the rod was approximately 100 °C below the temperature of the fiber but, due to the small view factor and lack of significant scattering within the fiber, it did not represent a major source of radiant flux. The temperature of the gas stream was measured with two 0.08-mm-diam noble metal thermocouple probes which were placed 3.2 mm downstream from the fiber. Due to the high mass rate of flow, the fiber temperature was within 1% of the measured gas temperature.[22]

Because the absorption within the fiber is small, the absorption coefficient $\alpha(T)$ can be approximated by

$$\alpha(T) = [-\ln(1 - E_f/E_b)]/x, \tag{5}$$

where x is 7.6 cm and the product αx is small, E_f is the radiance from the heated 7.6-cm section of the fiber, and E_b

is the radiance from a blackbody furnace at the same temperature as measured with the test fiber. Under conditions of local thermodynamic equilibrium that existed for this experiment, it is valid to apply Kirchoff's Law of Reciprocity[23] and equate the absorption coefficient to the emission coefficient.

At 800 nm, the ratio of the intensity of the blackbody radiance to the self-emission was greater than 300 over the entire temperature range measured. The absorption coefficient for the fiber used in the freezing-point experiments is shown in Fig. 8. There is a slight temperature dependence of the absorption at this wavelength. Between 850 and 1060 °C, the absorption coefficient is described by the empirical relationship

$$\alpha(T) = 1.895\times10^{-5}\exp[2.773\times10^{-3} \times(T+273.15)]\ \text{cm}^{-1}. \quad (6)$$

No data could be obtained below 850 °C because the intensity of the self-emission from the fiber was below the limit of detection of the radiometer. Therefore, in the analysis of the freezing-point data, $\alpha(T)$ was assumed to obey Eq. (6) above 850 °C and to remain constant at 4.3×10^{-4} cm^{-1} for all lower temperatures (see Fig. 8).

For the isothermal environment in the freezing-point cells, the temperature distribution along the sapphire fiber is given by

$$T(x) = T(l) + [T - T(l)]\left(1 - \frac{\cosh mx + \beta\sinh mx}{\cosh ml + \beta\sinh ml}\right), \quad (7)$$

where $T(l)$ is the temperature at the water-cooled end of the fiber which was measured to be 30 °C and T is the temperature of the well of the freezing-point cell which was assumed to be temperature of the freezing metal. In Eq. (7)

$$m = (4H/Kd)^{1/2} \quad (8)$$

and

$$\beta = H/Km, \quad (9)$$

where H is the convective heat transfer coefficient of the air in the well of the freezing-point cell, K is the thermal conductivity of the fiber, and d is the fiber diameter.[24] Equations (6) and (7) were used to supply the $T(s)$ and $\alpha[T(s)]$ values for Eq. (4). The correction to the silver freezing-point temperature for absorption in the sapphire fiber corresponded to -0.046 ± 0.022 °C.

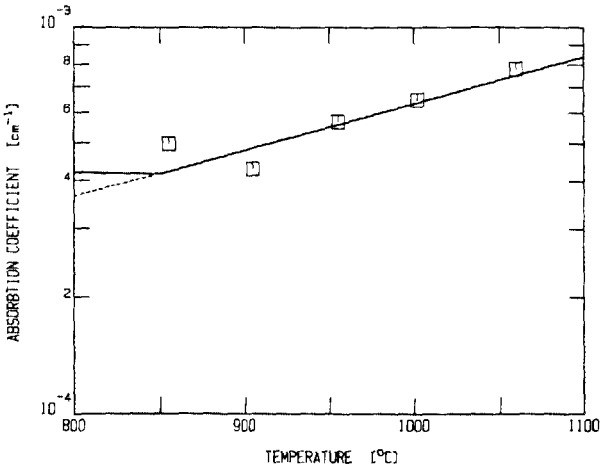

FIG. 8. Absorption coefficient vs temperature for the sapphire fiber used in this experiment [Eq. (6)]. Below 850 °C, the coefficient was assumed to have a constant value of 4.3×10^{-4} cm^{-1} as indicated by the solid line.

The sum of the scattering and absorption of radiant flux from the surface and the interior of the fiber was also examined in the combustor exhaust stream. The sapphire fiber of the OFT was again placed across the stream perpendicular to the axis of flow but 2.5 cm downstream from the exhaust nozzle. In this case, the fiber was surrounded by a hollow ceramic cylinder in which a 1.6-mm slit had been machined along its length. The slit was located at an angle of 45° from the stagnation point to enable the hot gases to heat the fiber within the cylinder. As before, the tip of the fiber extended beyond the cylinder and remained outside the flow. The temperature of the gas stream was measured with thermocouple probes both within the cylinder and 6.4 mm downstream from the cylinder.

Significant variations in the magnitude of both the scattering and absorption were observed between the several fibers tested but, in general, the output of the OFT due to scattering was less than that due to self-emission. If the output measured when the fiber was behind the ceramic rod was, in fact, due to scattering rather than self-emission, then, when the fiber was located within the cylinder, the output for similar conditions should have increased by a factor of 20 due to the increased view factor. For the fiber used in the freezing-point experiments, the amount of radiant flux scattered into the fiber from the ceramic cylinder was less than one-tenth of the emitted flux. In the isothermal cavity of the freezing-point cell such a small amount of scattering was not important.

E. Reflection losses at the air-to-fiber interfaces

The reflectivity of the heated end face of the high-temperature fiber varied with temperature. From data obtained in a subsequent experiment[25] it was determined that, at the temperature of the silver freezing point, the reflectivity at the air-to-sapphire interface was $0.35 \pm 0.05\%$ less than that at the temperature of the gold freezing point. A correction of -0.025 ± 0.004 °C was made in the silver freezing-point temperature due to this effect. It was assumed that the reflection loss at the cooled sapphire-to-silica interface and at the silica-to-air interface in the radiometer remained the same for the measurements in each freezing-point cell.

F. Impurity in the freezing-point cells

The gold freezing-point cell that was used in our experiment contained a sample that had been used in an earlier cell. It was believed that the freezing-point temperature of the cell was within 0.010 °C of the freezing temperature of pure gold.[26] This cell has subsequently been compared with a newly constructed cell containing NBS Standard Reference Material 685 which had an impurity content of less than one part per million. Results obtained with five high-temperature platinum resistance thermometers show that the freezing-point temperature realized in the cell that we used is 0.015 ± 0.002 °C lower than that of the new cell.[27] Assum-

TABLE I. The ratio of the radiance at the freezing point of gold to that at the freezing point of silver plus the associated silver freezing-point temperatures.

	L_{Au}/L_{Ag}	T_{Ag} (°C)
Predicted value	2.9999 ± 0.0005	961.980 ± 0.015
Experimental value	2.9995 ± 0.0006	961.99 ± 0.017
Corrected value	3.0029 ± 0.0011[a]	961.91 ± 0.030[a]

[a] Includes the uncertainty associated with the imprecision of the experimental value and correction for systematic errors.

ing, due to the high purity of the sample, that there was no lowering of the freezing-point temperature of the new gold cell, the correction for the impurity-lowered freezing-point temperature of the gold in the cell that we used and its reproducibility corresponded to -0.013 ± 0.002 °C in the silver-point temperature.

The silver freezing-point cell contained NBS Standard Reference Material 748 which had an impurity content of less than one part per million. Due to the high purity of the sample, it was also assumed that there was no lowering of the silver-point temperature. The uncertainty due to the reproducibility of the freezing-point temperature of the silver corresponded to ± 0.002 °C.

V. RESULTS

A comparison between the experimental and the predicted values for the ratio of the radiance at the freezing point of gold to that at the freezing point of silver L_{Au}/L_{Ag} is presented in Table I. The predicted value is that which would be expected using the Jones and Tapping value[11] for the silver freezing-point temperature (961.980 ± 0.015 °C), the value assigned to the impurity-lowered freezing-point temperature of the gold cell used in the present experiment (1064.415 ± 0.002 °C), and the independently measured spectral response of the radiometer when equipped with the 100-nm-wide interference filter centered at 800 nm (see Sec. IV A and Fig. 5). The predicted value also includes a correction for the effect of the hydrostatic pressure on the equilibrium temperature in each cell.

The corrected value for L_{Au}/L_{Ag} given in Table I is referred to the IPTS-68 temperature for the gold freezing point (1064.43 °C) and is the product of the experimental value for the ratio and the total correction factor given in Table II. The uncertainty is the square root of the sum in quadrature of the estimated systematic error in the experimental ratio and the error associated with the uncertainty in the correction factor. The silver freezing-point temperature corresponding to the corrected value of the radiance ratio is compared with other recent literature values in Fig. 9.

In Table I it is seen that the uncorrected experimental value for the radiance ratio is really quite close to the predicted value. The primary correction, corresponding to -0.046 °C (see Table II), is due to the absorption in the Al_2O_3 fiber; the large uncertainty in this correction can be reduced by the use of superior sapphire fibers and a freezing-point cell and furnace designed specifically for the OFT measurements. The uncertainty of the corrected value for the radiance ratio corresponds to ± 0.030 °C; this can be reduced with superior information on the temperature dependence of Al_2O_3 absorption, better definition of the spectral response of the radiometer, and superior experimental technique.

However, it is improbable that the detector nonlinearity will be defined to better than one part in 10^4 and, therefore, it can be expected that the practical accuracy of the OFT will

TABLE II. Summary of measurement errors.

Source of error	Radiance ratio		Silver freezing point	
	Correction	Uncertainty	Correction (°C)	Uncertainty (°C)
Radiometer				
Linearity	1.000104	± 0.000104	− 0.009	± 0.009
Filter transfer function				
Wavelength accuracy	1.000000	± 0.000058	0.000	± 0.005
Out-of-band transmission	1.000046	± 0.000046	− 0.004	± 0.004
Sapphire fiber				
Temperature dependence of Al_2O_3 absorption	1.000531	± 0.000257	− 0.046	± 0.022
Scattering	1.000000	± 0.000000	0.000	± 0.000
Temperature dependence of Al_2O_3 reflectivity	1.000290	± 0.000050	− 0.025	± 0.004
Fixed-point cells				
Gold: Impurity plus reproducibility	1.000149	± 0.000020	− 0.013	± 0.002
Hydrostatic head	1.000014	± 0.000000	− 0.001	± 0.000
Silver: Impurity plus reproducibility	1.000000	± 0.000020	0.000	± 0.002
Hydrostatic head	0.999990	± 0.000000	+ 0.001	± 0.000
Total	1.001124	± 0.000293	− 0.097 °C	± 0.025 °C

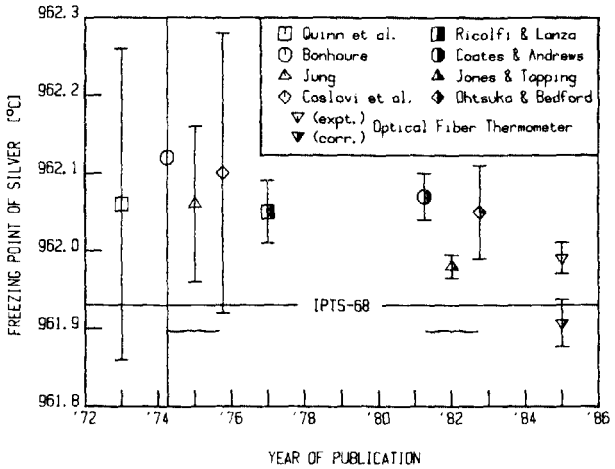

FIG. 9. A comparison between the corrected value for the temperature of the freezing point of silver as determined with the optical fiber thermometer, 961.91 ± 0.030 °C, and other recently published results. (Also plotted, for the convenience of the reader, is the temperature associated with the experimental value for radiance ratio.) The horizontal line at 961.93 °C is the value assigned on the International Practical Temperature Scale of 1968 (IPTS-68).[3] The published values are Quinn, Chandler, and Chattle[5]: 962.06 ± 0.2 °C; Bonhoure[6]: 962.12 ± 0.39 °C; Jung[7]: 962.06 ± 0.10 °C; Coslovi, Rosso, and Ruffino[8]: 962.10 ± 0.18 °C; Ricolfi and Lanza[9]: 962.05 ± 0.04 °C; Coates and Andrews[10]: 962.05 ± 0.03 °C; Jones and Tapping[11]: 961.980 ± 0.015 °C; and Ohtsuka and Bedford[12]: 962.07 ± 0.06 °C.

eventually be limited to about ± 0.010–0.015 °C near 1000 °C. That these initial experiments were within a factor of 2–3 of that limit indicates that the device can be relatively easily configured for practical temperature standards measurements. Research to improve the performance and evaluate the potential of the OFT as a new high-temperature standard instrument is continuing.

VI. CONCLUSION

The performance of the new optical fiber thermometer has been evaluated by determining the temperature interval between the gold and silver freezing points. It is important to note that the results given in this paper are based on only a single measurement at each freezing point and, although the measurements were conducted with care, not all the tests for systematic sources of error required for a definitive determination of the silver freezing-point temperature were conducted. As a consequence, the agreement between the value of the silver freezing-point temperature obtained in this experiment and recent values based upon more extensive measurements can only be considered as evidence of the potential accuracy of the OFT. However, it has been demonstrated that even with the limitations of these initial tests, the uncertainty is of the order of ± 0.030 °C, or 0.003%, near 1000 °C. Examination of the sources of error suggests that through improved experiment and device design, this error can ultimately be reduced by factor of 2 to 3.

ACKNOWLEDGMENTS

The authors wish to thank Bruce Dove and George Evans, Jr. for their assistance in constructing the radiometer; Frank Gibson and Steve Semancik for preparation of the fibers; Eli Liang, Russell Schaefer, Kenneth Eckerle, Edward Zalewski, and Victor Weidner for their help in the characterization of the optical properties of the fiber and the spectral response of the radiometer; John Evans for his assistance in the freezing-point measurements; and James Allen for his general help in apparatus construction and assistance during all of the experiments.

[1]R. R. Dils, J. Appl. Phys. **54**, 1198 (1983).
[2]T. P. Jones, Metrologia **4**, 80 (1968).
[3]H. Preston-Thomas, ed., Metrologia **12**, 7 (1976).
[4]E. H. McLaren and E. G. Murdock, Natl. Res. Council (Canada) Monograph NRCC 17407 (1979).
[5]T. J. Quinn, T. R. D. Chandler, and M. V. Chattle, Metrologia **9**, 44 (1973).
[6]J. Bonhoure, Metrologia **11**, 141 (1975).
[7]H. J. Jung, *Temperature Measurement 1975* (Institute of Physics, London, 1975), p. 278.
[8]L. Coslovi, A. Rosso, and G. Ruffino, Metrologia **11**, 85 (1975).
[9]T. Ricolfi and F. Lanza, High Temp.-High Pressures **9**, 483 (1977).
[10]P. J. Coates and J. W. Andrews, *Temperature, Its Measurement and Control in Science and Industry* (AIP, New York, 1982), Vol. 5, p. 109.
[11]T. P. Jones and J. Tapping, *Temperature, Its Measurement and Control in Science and Industry* (AIP, New York, 1982), Vol. 5, p. 169.
[12]M. Ohtsuka and R. E. Bedford, *Temperature, Its Measurement and Control in Science and Industry* (AIP, New York, 1982), Vol. 5, p. 175.
[13]J. P. Evans (private communication).
[14]H. E. LaBelle, Jr., J. Cryst. Growth **50**, 8 (1980).
[15]Certain commerical equipment and materials are identified in this paper in order to adequately specify the experimental procedure. Such identification does not imply recommendation or endorsement by the National Bureau of Standards, nor does it imply that the materials or equipment are necessarily the best available for the purpose.
[16]K. D. Mielenz, K. J. Eckerle, R. P. Madden, and J. Reader, Appl. Opt. **12**, 1630 (1973).
[17]W. Budde, Appl. Opt. **18**, 1555 (1979).
[18]T. J. Quinn and R. Lee, *Temperature, Its Measurement and Control in Science and Industry* (ISA, Pittsburgh, 1972), Vol. 4, p. 395.
[19]R. R. Dils and P. S. Follensbee, J. Eng. Power **99A**, 497 (1977).
[20]R. R. Dils and P. S. Follensbee, Corrosion **33**, 385 (1977).
[21]R. R. Dils and P. S. Follensbee, NBS Spec. Publ. 561 (1979), p. 1027.
[22]R. R. Dils and P. S. Follensbee, *Proceedings of the 21st International Instrumentation Symposium* (ISA, Pittsburgh, 1975), p. 127.
[23]H. P. Baltes, *Progress in Optics* (American Elsevier, New York, 1976), Vol. XIII, p. 1.
[24]E. R. G. Eckert, *Introduction to the Transfer of Heat and Mass* (McGraw-Hill, New York, 1950).
[25]J. Tapping and M. L. Reilly (to be published).
[26]J. P. Evans, *Temperature, Its Measurement and Control in Science and Industry* (AIP, New York, 1982), Vol. 5, p. 771.
[27]J. P. Evans (private communication).